The Tone Generator and Phase Calibration in VLBI Measurements

J. B. Thomas
Tracking Systems and Applications Section

In very long baseline interferometry (VLBI) applications, the measurements of geophysical/astrometric quantities and clock synchronization are degraded by unknown and unstable phase effects due to instrumentation. Most of these phase effects can be removed through the use of a tone generator that injects near the front of the instrumentation a set of tones derived from the station frequency standard. When properly used, such a calibration technique will not only remove post-injection instrumental phase instabilities, but will also allow absolute calibration of interferometer phase so that clock synchronization is possible. As implied, these advantages of the tone generator pertain only to instrumental effects after the injection point. This report presents a nonrelativistic mathematical model to describe the calibration signal, its processing, and its use in removing instrumental effects from interferometer phase.

I. Introduction

In very long baseline interferometry (VLBI) measurements, the measured delays are corrupted by unknown and unstable phase shifts due to instrumentation. Such phase effects can degrade the accuracy of geophysical measurements and complicate measurements of clock synchronization. Most of these instrumental effects in VLBI measurements can be removed through the use of a phase calibrator. The commonly used approach, pioneered by A. E. E. Rogers (Ref. 1), is to inject at a point near the front of the instrumentation a calibration signal consisting of a set of tones, equally spaced in frequency and derived from the station frequency standard. When properly used, such a calibration technique will not only correct for system phase instabilities, but will also allow absolute calibration of interferometer phase so that clock synchronization is possible. Phase calibration hardware, suitable for use in the Deep Space Network, is currently being developed at the Jet Propulsion Laboratory in Division 33 (R. L. Sydnor's group).

It should be noted that the aforementioned advantages of phase calibration pertain only to instrumental effects after the calibrator injection point and that other measures must be taken to account for instrumental effects before that point. This report will ignore the important issue of calibration before the injection point.

As implied above and indicated in the text, the goal of phase calibration is to remove from the phase all instrumental effects after the injection point so that the measured values of delay and delay rate are left in their ideal form: a sum of geometric delay and clock offset terms. (For simplicity, transmission media terms will be ignored). In this report, a nonrelativistic model is developed to describe the tone signal, its processing, and its use in removing instrumental effects.

The sections dealing with phase analysis are similar to an analysis by Fanselow (Ref. 2), but are more detailed. Further, material has been added that deals with clock modeling, tone amplitude, and tone SNR.

The sections in this report have been organized as follows: Section II models the calibrator signal including power level, clipping, tone-stopping, and stopped-tone SNR. Section III presents fundamental definitions in clock modeling. Section IV develops a detailed model for the amplitude and phase of the calibrator signal in terms of basic instrumental effects. Section V presents a heuristic derivation of interferometer phase in terms of basic instrumental effects. Section VI demonstrates formally how the calibration process removes instrumental effects from interferometer phase. Section VII summarizes areas where work remains to be done.

II. Phase Calibrator Signal

This section treats the phase calibrator signal and includes an analysis of: (a) tone power (b) the effect of bilevel clipping on the recorded signal (c) tone stopping (d) stopped-tone SNR. Since it is not necessary for these topics, this section will not decompose tone phase and amplitude into more fundamental quantities but will treat each of them as a single variable. Section IV will deal with the more complicated problem of expressing tone amplitude and phase in terms of contributing instrumental factors.

The phase calibrator injects near the front of the instrumentation an equally spaced set of tones that have all been derived from the same frequency standard. The phases of these tones are expected to be stable at the 10-picosecond level and calibrated absolutely to the nanosecond level. Each channel bandpass will probably contain more than one tone, but determination of the optimum number will require a thorough study of bandpass characteristics, a task outside the scope of this report. The calibrator signal will be injected into the system at a low power level and thus imbedded in the radio source data. The Mark II system digitally records the signal in a bilevel mode at 4 Mbits/sec. Each tone will be extracted at the correlator by mixing the bit stream digitally with a frequency that closely approximates the baseband frequency for that tone.

The analog baseband signal (before clipping) can be represented in the form

$$V(t) = S(t) + \sqrt{T_s}\, W(t) \tag{1}$$

$$= \sum_n A_n \cos \phi_n(t) + \sqrt{T_s}\, W(t) \tag{2}$$

where the calibrator signal (S) has been decomposed in the second equation into its constituent tones. As implied above, the baseband phase (ϕ_n) of each tone will be essentially linear in time. We have normalized the noise term W, which contains both system noise and radio source noise, to unity [i.e., $\langle W^2 \rangle = 1$]. The factor T_s is the (average) system temperature contributed by W.

Total power of the signal will be given by

$$P \propto \langle V^2 \rangle = \frac{1}{2} \sum_n A_n^2 + T_s \tag{3}$$

If we specify total calibrator power relative to total noise power, we can express the tone amplitude in terms of T_s. That is, if the ratio of total calibrator power to total noise power is ϵ, then the ratio (SNR) of tone amplitude to rms noise voltage becomes

$$\boxed{\frac{A}{\sqrt{T_s}} \approx \sqrt{\frac{2\epsilon}{N_c}}} \tag{4}$$

where N_c is the number of tones in the passband, and A is the (virtually constant) tone amplitude within the passband. (It is unnecessary for our purposes to resolve the minor ambivalence involving tones on the bandpass edges.) We currently plan to keep the total calibrator power low – say, 2% of the system noise. Thus, if there are 3 tones in the passband, the SNR for a tone becomes

$$\frac{A}{\sqrt{T_s}} \approx \sqrt{\frac{2 \times 0.02}{3}} \approx 0.12 \tag{5}$$

(For the sake of numerical example, we will assume a nominal system with a 2% power level and 3 tones/passband. It is outside the scope of this work to determine optimum values for these parameters.) It is worth noting here that this "single-sample" SNR is large compared to typical intercontinental cross-correlation amplitudes, which are usually in the range 0.001 to 0.04. The tone SNR in Eq. 4 will be modified slightly below when two-level sampling is taken into account and will increase when many bits are collected in the tone-stopping process.

The maximum value of the total tone signal S will occur whenever all tones are in phase and is given by

$$\frac{S_{max}}{\sqrt{T_s}} \approx N_c \frac{A}{\sqrt{T_s}} \tag{6}$$

This maximum value occurs, of course, every time a calibrator pulse (see Section IV) reaches the recorder and equals about 0.35 for the example above. (The pulse width at baseband is approximately equal to inverse of the system bandwidth when a number of tones are in the passband.)

We are now prepared to analyze tone-stopping in the correlator. Let $\tilde{V}_k$ be the recorded signal at time t_k, where the tilde denotes bilevel sampling. For a given station the correlator will counter-rotate (tone-stop) a given tone as follows

$$V_{sn} = \frac{1}{N_t} \sum_{k=1}^{N_t} \tilde{V}_k \exp -i\psi_{nk} \tag{7}$$

where ψ_{nk} is the model phase for the n^{th} tone at time t_k. (In this report, we will not take into account the fact that the Mark II correlator uses a trilevel quantized model for the stopping sinusoids. Such trilevel quantization has only two minor effects: a slight decrease in SNR and a change in stopped-fringe (or tone) amplitude. In tone analysis, these changes are not significant in most applications. However, if absolute calibration of tone amplitude is desired, this amplitude effect must be considered. Overall phase is not affected by such quantization.)

We will now calculate the expectation value of the stopped tone given in Eq. 7. Unlike interferometric cross-correlation where both the signal and noise are random, the tone signal is deterministic and the "noise" $W(t)$ is random (see Eq. 1). The expectation of Eq. 7 becomes

$$\langle V_{sn} \rangle = \frac{1}{N_t} \sum_{k=1}^{N_t} \langle \tilde{V}_k \rangle \exp(-i\psi_{nk}) \tag{8}$$

The expectation for a single sample point $\tilde{V}_k$ can easily be calculated as follows:

$$\langle \tilde{V}_k \rangle = \int_{-\infty}^{\infty} Q(V)P(V)dV \tag{9}$$

where

$$Q(V) = +1, \; V > 0$$

$$= -1, \; V < 0$$

and where the probability distribution of V (about S) is given by

$$P(V) = \frac{1}{\sqrt{2\pi T_s}} \exp\left[-(V-S)^2/2T_s\right] \tag{10}$$

The tone signal S is defined in Eq. 1. This integral can be shown to equal

$$\langle \tilde{V}_k \rangle = \sqrt{\frac{2}{\pi}} \int_o^{S/\sqrt{T_s}} \exp(-z^2/2)\, dz \tag{11}$$

$$\approx \sqrt{\frac{2}{\pi}} \left[\frac{S}{\sqrt{T_s}} - \frac{1}{6}\left(\frac{S}{\sqrt{T_s}}\right)^3 + \ldots \right] \tag{12}$$

$$\approx \sqrt{\frac{2}{\pi}} \frac{S}{\sqrt{T_s}} \tag{13}$$

if one neglects higher order terms. As indicated above, the maximum of $S/\sqrt{T_s}$ in our nominal system will be about 0.35 so that the maximum of the cubic term will be of the order of 2% relative to the first term (before tone stopping). This cubic term can be represented as a sum of three-tone beat notes. During tone-stopping, a given three-tone beat note will clearly be reduced to an insignificant level provided it possesses a different frequency than the original tone frequencies. If this last condition is not satisfied, a given offending three-tone beat note in a system with $A/\sqrt{T_s} = 0.12$ would fractionally contribute in amplitude:

$$\frac{1}{8} * \frac{1}{6} \left(\frac{A_n}{\sqrt{T_s}}\right)^2 \lesssim 0.0003 \tag{14}$$

or 0.03% to the tone under consideration. Although this is not much by itself, many equally spaced tones can generate many three-tone beat notes equal to a given original tone frequency.

Thus the combined effect might be non-negligible when there are many tones in the passband. This problem will deserve more thorough study if many tones are ever used.

Based on Eq. 13 and the decomposition of S in Eq. 2, the stopped tone in Eq. 8 thus becomes

$$\langle V_{sn} \rangle = \frac{1}{\sqrt{2\pi}} \frac{A_n}{\sqrt{T_s}} \exp\left[i(\phi_n - \psi_n)\right] \qquad (15)$$

if we assume the other tones sum to negligible levels. The phase difference $\phi_n - \psi_n$, presumed to be nearly constant, is the phase difference at the middle of the sum interval. (We will assume stopped-tone frequency is negligibly small. If it is not, there are straightforward, simple ways to overcome the difficulty).

The noise on the stopped tone due to system noise can be calculated as follows:

$$\sigma_V^2 = \left\langle \left(V_{sn}^R - \langle V_{sn}^R \rangle \right)^2 \right\rangle \qquad (16)$$

where V_{sn}^R is the real part of the stopped tone in Eq. 7. Using Eq. 7, one obtains

$$\sigma_V^2 = \frac{1}{N_t^2} \sum_{k\ell} \left[\langle \tilde{V}_k \tilde{V}_\ell \rangle - \langle \tilde{V}_k \rangle \langle \tilde{V}_\ell \rangle \right] \cos \psi_{nk} \cos \psi_{n\ell} \qquad (17)$$

These expectation values can be evaluated to obtain

$$\sigma_V^2 \approx \frac{1}{2N_t} \left[1 + \frac{2}{\pi} \sum_{\tau \neq 0} R(\tau) \cos 2\pi \nu_n \tau \right] \qquad (18)$$

where $R(\tau)$ is the bitstream autocorrelation function, and ν_n is the baseband frequency of the n^{th} tone. The derivation of this expression assumes that interbit correlations of system noise are small. The first term represents the noise that would be present if there were no correlation between bits. The second term accounts for small correlations between bits and will be of the order of 10% or less, but the exact size depends on the shape of the bandpass, the sample rate relative to bandwidth, and the value of the baseband tone frequency ν_n. Note that, if the small second term is neglected, the tone noise is the same for all tones.

We can now calculate the stopped tone SNR using Eqs. 4, 15, and 18. The SNR will be defined as the maximum amplitude (modulus) of the stopped tone divided by the rms noise:

$$\text{SNR} = \frac{1}{\sqrt{2\pi}} \frac{A_n}{\sqrt{T_s}} \frac{1}{\sigma_V} \qquad (19)$$

$$\boxed{\text{SNR} \approx \sqrt{\frac{2\epsilon N_t}{\pi N_c}}} \qquad (20)$$

where we have neglected the small interbit-correlation term in Eq. 18. In analogy with fringe phase calculations, the system noise error in the calibration phase will be

$$\sigma_\phi = \text{SNR}^{-1} \qquad (\text{SNR} \gg 1) \qquad (21)$$

The following example will help illustrate the size of the system noise error in the phase calibrator corrections. As assumed above, suppose we have a 2% total power level for the calibrator signal with 3 tones across the passband. When 4 seconds of MKII data (record rate = 4 Mbs) are reduced for a given tone, we obtain from Eq. 20

$$\text{SNR} \approx \sqrt{\frac{2 \times .02 \times 4 \times 4 \times 10^6}{3\pi}} \approx 260 \qquad (22)$$

The associated phase error will be

$$\sigma_\phi \approx \frac{1}{260} \text{rad} = 0.0006 \text{ cycle} \qquad (23)$$

This phase error would be the system noise error in the phase from one tone. When fringe phase is calibrated, a number of tones (N_u) in the passband will probably be used, in which case the system noise error in the overall phase would be

$$\boxed{\sigma_\phi^T \approx \frac{\sigma_\phi}{\sqrt{N_u}} \approx \sqrt{\frac{\pi}{2N_t\epsilon} \frac{N_c}{N_u}}} \qquad (24)$$

For our numerical example, the overall phase error becomes

$$\sigma_\phi^T \approx 0.00035 \text{ cycle} \tag{25}$$

if all 3 tones are used. For a 40-MHz spanned bandwidth in a bandwidth-synthesis delay measurement, the corresponding delay error will be

$$\sigma_\tau = \frac{\sqrt{2} \times 0.00035 \text{ cycle}}{40 \text{ MHz}} = 0.012 \text{ nsec} = \frac{0.36 \text{ cm}}{c} \tag{26}$$

The factor of $\sqrt{2}$ is a result of the combination of two channels in the BWS process.

III. Clock Model

Before proceeding to detailed calibrator analysis, it is advisable to specify some rather trivial time-keeping terms that are a potential source of confusion if left undefined. First, we will define the following symbols:

t = true (universal) time

t_c = station (universal) time (station clock)

ω_o = true oscillator frequency (in terms of true time)

ω_c = nominal oscillator frequency (e.g., 5 MHz)

The phase ϕ_c of the station oscillator is the quantity that physically exists and is measured for the purpose of timekeeping. By definition, the oscillator phase at the selected clock reference point will be given in terms of true time and frequency by

$$\phi_c = \omega_o (t - t_o) \tag{27}$$

where t_o is a reference time. By design, clock synchronization will be referred to this point.

When the phase ϕ_c of the station oscillator is measured at this point, station time can be operationally defined and determined by

$$t_c \equiv \phi_c / \omega_c \tag{28}$$

We assume here that t_c is zero when ϕ_c is zero. This is possible since a particular zero crossing can be defined to be UT = 0.

If the nominal frequency is related to the true frequency by

$$\omega_o = \omega_c + \Delta\omega_c \tag{29}$$

then station time is related to true time by

$$t_c = t + \tau_c \tag{30}$$

where the clock error τ_c for that station is given by

$$\tau_c = \frac{\Delta\omega_c}{\omega_c}(t - t_o) - t_o \tag{31}$$

Usually the difference between ω_c and ω_o is small, less than a part in 10^{11}.

The following analysis will use some simple time relations that should be explicitly specified. Let t_{bj} represent the time marked off on the tape by the bits at station j and let τ_{rj} represent the cable delays, etc., from the clock to the sampler. Then bit time is related to station time by

$$t_{bj} = t_{cj} - \tau_{rj} \tag{32}$$

and, based on Eq. 30, to true time by

$$t_{bj} = t_j + \tau_{bj} \tag{33}$$

where

$$\tau_{bj} \equiv \tau_{cj} - \tau_{rj} \tag{34}$$

(We should note here that we have simplistically assumed that the timing signal for the sampler originates at the clock reference point discussed above. The fact that this will not necessarily be the case is not important as far as phase calibration is concerned. A separate point of origin for the sampler timing signal would simply result in a different value for timing signal delay τ_r. As we shall see, τ_r, whatever its origin or value, is removed in phase calibration.)

IV. Detailed Model for Tone Amplitude and Phase

In this section, calibrator phase is broken down in terms of the various effects that enter the calibrator signal in

transit from the clock through the instrumentation and then through the data reduction procedure. Since the analysis will be based on an "ideal" model for the system, extra effort might be required to account for some deviations from ideal behavior. It is beyond the scope of this report to assess all complications – as we shall see, even the analysis of the ideal system is fairly involved.

The analysis that follows develops the model for the calibrator signal in the following sequence: it models effects on the signal (a) from the clock to the injection point, (b) from the injection point to the recorder and (c) through the data reduction procedure. The simplified block diagram of the instrumentation shown in Fig. 1 will be useful in tracing the signal through the instrumentation.

First, for step (a), the phase of the signal at the clock reference point (i.e. the output of the cable stabilizer in Fig. 1) will be given in terms of true time and nominal frequency by

$$\phi_c = \omega_c(t + \tau_c) \tag{35}$$

as indicated by Eqs. 28 and 30. We have chosen to represent calibration phase in this way since a) the clock error τ_c is explicitly shown b) true time t is a scale common to both stations, and c) tone frequencies will be calculated by the correlator operator on the basis of the nominal frequency ω_c. The clock signal will experience a cable delay (τ_u) so that its phase entering the tone generator will be given by

$$\phi_c = \omega_c(t + \tau_c - \tau_u) \tag{36}$$

The "ideal" tone generator will detect the zero crossings of the input signal and convert the positive-going zero crossing into rectangular pulses as schematically indicated in Fig. 2. We currently plan to make the width (τ_p) of the output pulses equal to about 20 psec. Different (slower than ω_c = 5 MHz) repetition rates will be obtained by blanking pulses. For example, by passing every 10th pulse, the pulse repetition rate would be 500 kHz. The passed repetition rate will be denoted by ω_p. As indicated below, the tone frequencies will be the harmonics of the fundamental repetition rate ω_p.

In practice, there will be deviations from the ideal waveforms shown in Fig. 2, deviations such as delays, phase shifts and an amplitude distortion, arising in both the tone generator and connecting elements. For example, we have assumed that a zero crossing is at the center of a rectangular pulse. In practice, this is not necessarily precisely the case but can be accounted for. Further, the pulse shapes will not be perfect rectangles. This report will not consider such deviations but will note that most of these effects can be formally included by making a complex Fourier expansion rather than the cosine expansion presented below. However, we will note here that a constant deviation from rectangularity will cause clock synchronization measurements to be biased by a constant error that is less than the pulse width. Further, a constant deviation will cause no error in geophysical/ astrometric measurements.

The ideal calibrator signal in Fig. 2 can be Fourier decomposed to give

$$S(t) = C \sum_{n=1}^{\infty} F_p(\omega_n) \cos [\omega_n (t + \tau_c - \tau_u)] \tag{37}$$

where, for simplicity, we have neglected a constant term that is of no importance due to subsequent filtering. The tone frequency ω_n is a multiple ($n\omega_p$) of the nominal pulse rate ω_p. The function F_p is the Fourier transform of an individual rectangular pulse and is given by

$$F_p(\omega) = \frac{\sin \omega\tau_p/2}{\omega\tau_p/2} \tag{38}$$

Note that the phase of the Fourier components is consistent with the placement of the positive-going zero crossings at the rectangle centers. With a pulse width of 20 psec, the tone amplitude at X-band (8.4 GHz) will fall off to about

$$F_p(\omega_x) \approx 1 - \frac{(\omega_x\tau_p/2)^2}{6} \approx 0.95 \tag{39}$$

or a loss of about 5% relative to the maximum amplitude at lower frequencies. The amplitude change across the passband at S- or X-band will be even smaller. For example, if the passband is 100 MHz, the amplitude change will be about 0.1% across the band at X-band. Thus, changes in tone amplitude across the passband due to pulse shape appear to be negligible.

We are now prepared to model effects on calibrator phase in transit from the injection point to the recorder and then through the tone-stopping process. As indicated in Eq. 37, the tone phase at the injection point will be given by

$$\phi_n = \omega_n(t + \tau_c - \tau_u) \tag{40}$$

We have not explicitly represented the small delays from the input of the tone generator to the injection point since these can be included in τ_u.

After injection, the signal at station j passes through various filters and is heterodyned to baseband under the combined effect of various mixing signals. The phase effects of all of the intervening components can be divided into three major categories. First, the overall effect of the mixing signals can be described as one total mixing signal, to be represented by $\omega_{hj} t_j + \phi_{hj}$, where ω_{hj} is the total mixing frequency and ϕ_{hj} accounts for a constant phase term as well as variations in mixing phase that are nonlinear in time. All group delays, including effective group delays through filters, will be represented by one total delay τ_{Ij}. All phase shifts (except those from group delays) will be represented by one total shift ϕ_{Ij}. Given these definitions, the tone phase at baseband will be equal to the injection phase (Eq. 40) combined with these three terms:

$$\phi_{nj}(t_{bj}) = \omega_n(t_j + \tau_{tj}) - \omega_{hj} t_j - \phi_{hj} - \omega_n \tau_{Ij} - \phi_{Ij}(\omega_n) \tag{41}$$

where

$$\tau_{tj} \equiv \tau_{cj} - \tau_{uj} \tag{42}$$

and where t_j is the true time corresponding to bit time t_{bj}. Fig. 1 schematically shows these modifications to calibrator phase on a step-by-step basis as the signal progresses through the instrumentation from clock to recorder. For clarity, however, the block diagram has been simplified to involve only one element of a given type and token phase shifts and group delays. Nevertheless, Eq. 41 is quite general if the variables are properly defined to account for lumped effects of all the elements in an actual system. At the correlator the operator will use a best estimate for the baseband frequency of each calibrator tone to separately "fringe-stop" each tone in a given bitstream. That is, in effect, the correlator will subtract from the phase of the n^{th} tone the phase

$$\psi_{nj} = (\omega_n - \omega'_{hj}) t_{bj} \tag{43}$$

$$= (\omega'_n - \omega'_{hj}) (t_j + \tau_{bj}) \tag{44}$$

where ω'_{hj} is the best (nominal) estimate for the heterodyne frequency and t_{bj} is bit time (Eq. 33) at station j.

The stopped calibrator phase (Eq. 15) at station j becomes

$$\Delta\phi_j(\omega_n) = \phi_{nj} - \psi_{nj} \tag{45}$$

$$= \omega_n(\tau_{tj} - \tau_{bj}) - \omega_n \tau_{Ij} - \phi_{Ij}(\omega_n) - \Delta\phi_{hj} \tag{46}$$

where the "stopped" heterodyne phase is given by

$$\Delta\phi_{hj} = \omega_{hj} t_j + \phi_{hj} - \omega'_{hj} t_{bj} \tag{47}$$

This puts the stopped-tone phase in the form we want, expressed in detail in terms of contributing effects due to instrumentation and data reduction.

V. Interferometer Phase

This section derives a theoretical expression for interferometer phase that includes most of the terms that enter VLBI measurements. However, since a full treatment of interferometry theory would exceed the scope of this report, we will only present a heuristic derivation based on a deterministic analog model for a single frequency component. As in the case of the calibrator signal, one can use the schematic block diagram in Fig. 1 as an aid in understanding the instrumental effects described below.

When the following sections deal with some instrumental terms, the same symbol will be used to denote the difference between stations as was used to denote the single station effect [e.g. τ_c and τ_u]. Consideration of the context of the equation should prevent confusion in interpretation.

Let the radio signal received at the calibrator injection point at station i be given by

$$V_i \propto \cos(\omega t + \theta) \tag{48}$$

where t is true time and ω is the radio frequency. The corresponding phase at station j will be delayed by a geometric delay τ'_g (referenced to the tone injection points) and will be given by

$$V_j \propto \cos[\omega(t - \tau'_g) + \theta] \tag{49}$$

As in the case of the calibration signals (Eq. 41), the instrumentation will contribute various phase terms in bringing these two signals to baseband:

$$V_i \propto \cos[\omega t + \theta - \omega_{hi} t - \phi_{hi} - \omega\tau_{Ii} - \phi_{Ii}] \quad (50)$$

$$V_j \propto \cos[\omega(t - \tau'_g) + \theta - \omega_{hj} t - \phi_{hj} - \omega\tau_{Ij} - \phi_{Ij}] \quad (51)$$

These signals are then sampled and recorded on magnetic tape at each station on the basis of the recorder timing (i.e. bit time). When the tapes are brought together for processing, the correlator will offset the signal at station j by a model delay τ_m and then multiply the two signals together to obtain

$$V_i(t_{bi}) V_j(t_{bj} + \tau_m) \propto \quad (52)$$

$$\cos[\omega(\tau'_g + \tau_b + \tau_I - \tau_m) + \phi_I + \Delta\theta_h + \omega_{hj}\tau_m]$$

where

$$\Delta\theta_h = \omega_{hj} t_j + \phi_{hj} - \omega_{hi} t_i - \phi_{hi} \quad (53)$$

$$\tau_I = \tau_{Ij} - \tau_{Ii} \quad (54)$$

$$\phi_I = \phi_{Ij} - \phi_{Ii} \quad (55)$$

$$\tau_b \equiv t_i - t_j = \tau_{bj} - \tau_{bi} \quad (56)$$

and where t_k is the true time corresponding to bit time t_{bk} at station k (see Eq. 33). The relation for $t_i - t_j$ depends on the correlator-enforced assumption that nominal bit times are correct (i.e. $t_{bi} = t_{bj}$). In this expression, we have only retained the difference-phase term in the cosine product rule since the sum-phase term will possess a high frequency and will average to negligible levels in subsequent time averaging. We should note that the reason for offsetting by τ_m in the above product is not obvious in the deterministic single-frequency derivation described here. A more general derivation would show (e.g. Ref. 3) that when the signals are derived from a random broadband process, they must be aligned in time to produce a correlated output.

After multiplication, the correlator will digitally heterodyne (counter-rotate or fringe-stop) the product signal (fringes) and thereby subtract a model phase given by

$$\phi_m = \omega'_{hj} t_{bj} - \omega'_{hi} t_{bi} + \omega'_{hj} \tau_m \quad (57)$$

The stopped signal will thus possess very low frequency ($\lesssim$50 mHz) and can be averaged over relatively large time intervals (0.1 - 1.0 sec). These stopped and averaged fringes will be given by

$$\sum_t V_i(t_{bi}) V_j(t_{bj} + \tau_m) \cos\phi_m$$

$$\propto \cos[\omega(\tau'_g + \tau_b + \tau_I - \tau_m) + \phi_I + \Delta\phi_h] \quad (58)$$

where

$$\Delta\phi_h \equiv \Delta\phi_{hj} - \Delta\phi_{hi}$$

and where we have assumed the sum-phase term averages to zero. Phase-tracking is then used to extract the fringe phase, given by

$$\boxed{\psi_f = \omega(\tau_g + \tau_a + \tau_b + \tau_I - \tau_m) + \phi_I + \Delta\phi_h} \quad (59)$$

where we have now represented the geometric delay in the customary fashion, $\tau'_g = \tau_g + \tau_a$. This redefines the geometric delay in terms of arrival times at the intersection of axes (i.e. τ_g) and adds a compensating term (τ_a) to account for the difference in pathlength for the radiowave in its actual propagation to the tone injection point and its theoretical propagation to the intersection of axes.

VI. Calibration of Interferometer Phase

This section demonstrates how the tone phase can be used to remove post-injection instrumental effects from the phase measured by the interferometer. As suggested in Fig. 1, the essence of phase calibration with tones is that all of these instrumental terms (except for τ_a) enter the tone phase in the same way that they enter the radio phase since both signals pass simultaneously through the same instrumentation and are simultaneously recorded by the same recorders. Thus, by subtracting the tone phase from interferometer phase, we can remove these instrumental terms.

Phase calibration will be applied as follows. For each station, tone phase is extracted from the stopped tones given by Eq. 15 (for example, by computing the inverse tangent of the ratio of real and imaginary parts). If we difference the measured tone phase between stations, we obtain

$$\phi_t(\omega) \equiv \Delta\phi_i(\omega) - \Delta\phi_j(\omega) \tag{60}$$

which, according to Eq. 46, is given theoretically by

$$\phi_t(\omega) = \omega(\tau_b + \tau_I - \tau_t) + \phi_I + \Delta\phi_h \tag{61}$$

where

$$\tau_t = \tau_{t_j} - \tau_{t_i}$$

We have assumed here that the calibration phase at a given frequency ω can be obtained by interpolation (or some other process) from the measured phases of the tones. Further, we neglect small doppler-shift effects, which produce frequency shifts of the order of a hundredth of a bandwidth but can be accounted for. When this calibration phase is subtracted from the fringe phase (Eq. 59), we obtain

$$\psi(\omega) = \psi_f - \phi_t \tag{62}$$

which is given theoretically by

$$\boxed{\psi(\omega) = \omega(\tau_g + \tau_c + \tau_a - \tau_u - \tau_m)} \tag{63}$$

where we have used Eq. 42 to show explicitly the clock-synchronization offset τ_c and the cable delay τ_u. We have now obtained a measurement of interferometer phase that is free of the instrumental terms calibrated by tone phase.

Once the interferometer phase has been corrected with tone phase, one can readily obtain the delay by the bandwidth synthesis (BWS) technique of taking the difference between the phases at frequencies ω_a and ω_b:

$$\tau'_{BWS} = \frac{\psi(\omega_a) - \psi(\omega_b)}{\omega_a - \omega_b} \tag{64}$$

which is given theoretically by

$$\tau'_{BWS} = \tau_g + \tau_c + \tau_a - \tau_u - \tau_m \tag{65}$$

Station calibration will provide measurements of the cable delay τ_u and intersection-of-axis delay τ_a so that they can be removed. The model delay τ_m is very accurately known, of course, and can be removed exactly. Thus, we finally obtain the desired quantity – a measured delay containing only geometric delay and clock offset:

$$\tau_{BWS} = \tau'_{BWS} - \tau_a + \tau_u + \tau_m \tag{66}$$

which is given theoretically by

$$\boxed{\tau_{BWS} = \tau_g + \tau_c} \tag{67}$$

The clock offset τ_c is the only remaining instrumental term. This term represents the synchronization offset between station clocks ($\tau_{cj} - \tau_{ci}$) and pertains to the clock reference points, established by the definition and removal of the cable delays, τ_u.

(We should note here that the aforementioned DSN calibrator system will have the capability of compensating on-site for the cable delay up to the tone generator by applying a calibrated advance to the phase leaving the cable stabilizer. In this case, τ_u in earlier equations would be equal to the small delay through the tone generator up to the injection point.)

As indicated previously, certain conditions must be met for this calibration analysis to be valid. First, the model for the heterodyne phase must be identical in the model phases used for fringe-stopping and tone-stopping. The calibrator signal must possess a low fractional power level. Tone frequencies must be chosen to handle phase variations across each channel passband, if such variations are present at a significant level.

In the calibration process described above, a subtle point has been neglected. Only the fractional part (in cycles) of both the interferometer phase and tone phase can be determined when phase is extracted after counter-rotation. The integer-cycle part of phase can not be determined by this process alone. Thus, when tone phase is subtracted from interferometer phase, the subtraction actually denotes removal of the fractional part of instrumental phase. We can ignore all integer cycle errors at this point since we realize that there are integer cycle ambiguities due to delay modeling that must be resolved later in the BWS process. The BWS process only requires as input precise values for the fractional part of phase, free of unwanted instrumental phase (fractional part). The integer-cycle part (due to τ_g and τ_c) is then added in a recursive process to be described in a later report. The output is a delay measurement free of post-injection instrumental

effects. It is a peculiarity of this technique that, even though delay and interferometer phase can be ultimately calibrated absolutely with regard to instrumental effects, instrumental phase, including integer cycles, is never absolutely measured.

VII. Remaining Work

Some important issues related to system calibration remain to be considered. For lack of adequate information concerning system characteristics (e.g., phase ripple and variability), this report has made no effort to assess the accuracy with which system calibrations can be carried out. This is obviously a crucial question that should be addressed as soon as possible. Such an accuracy analysis would have to consider the approximations, if any, that are imposed by practical considerations during implementation and will be intimately connected with the determination of the optimum number of tones and power level.

References

1. A. E. E. Rogers, "A Receiver Phase and Group Delay Calibrator for Use in Very Long Baseline Interferometry," Haystack Observatory Technical Note 1975-6.
2. J. L. Fanselow, "The Use of a Phase Calibrator in VLBI to Remove Receiving System Phase Shifts," JPL IOM 315.2.011 (an internal document), Oct. 1976.
3. J. B. Thomas, "An Analysis of Long Baseline Radio Interferometry," JPL DSN Progress Report 32-1526, Vol. V (1971).

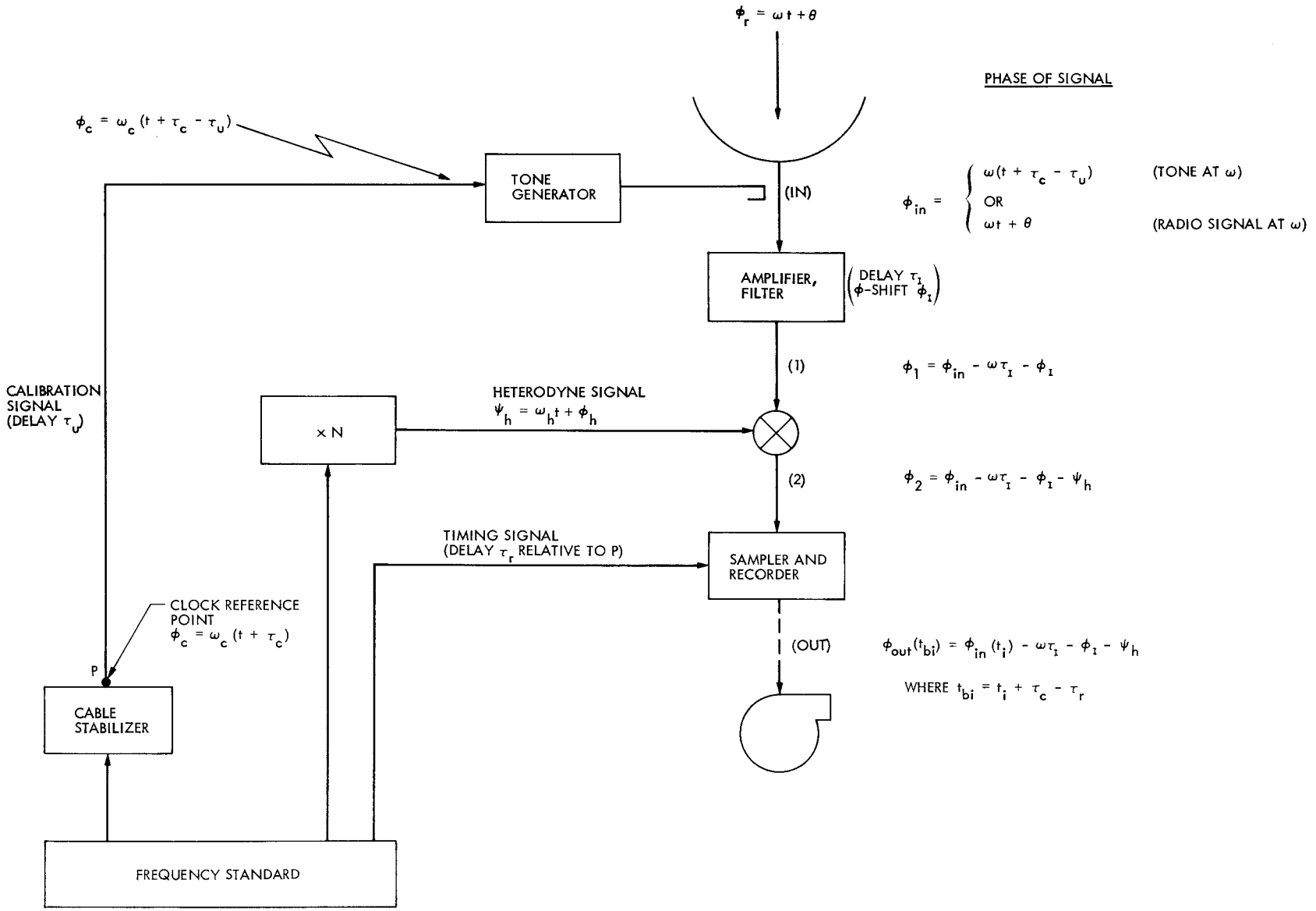

Fig. 1. Simplified illustration of VLBI instrumentation

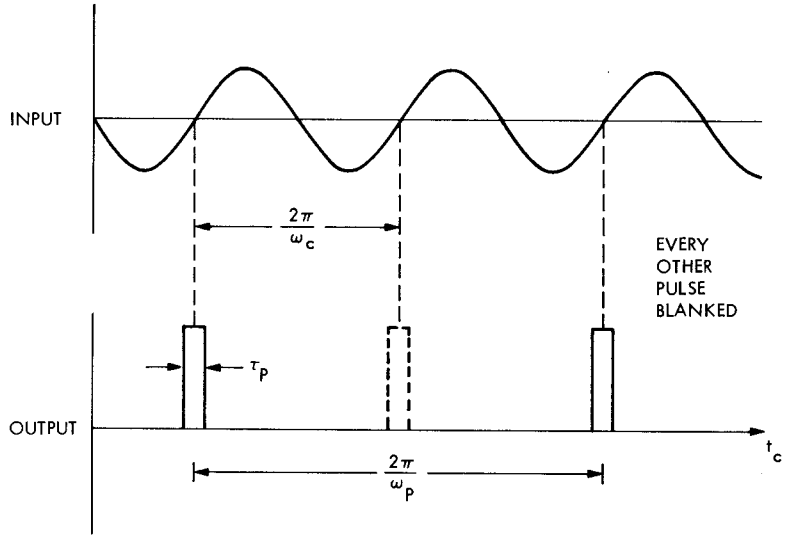

Fig. 2. Input and output signals for an ideal tone generator